[1.1.1.1]- and [2.2.1.1]Pagodane Dications: Frozen Two-Electron Woodward-Hoffmann Transition-State Models[1]

G. K. Surya Prakash,† V. V. Krishnamurthy,† Rainer Herges,† Robert Bau,† Hanna Yuan,† George A. Olah,*,† Wolf-Dieter Fessner,‡ and Horst Prinzbach*,‡

Contribution from the Donald P. and Katherine B. Loker Hydrocarbon Research Institute and Department of Chemistry, University of Southern California, Los Angeles, California 90089-1661, and Chemisches Laboratorium der Universität Freiburg im Breisgau, Institut für Organische Chemie und Biochemie, Albertstrasse 21, D-7800 Freiburg, FRG.
Received March 18, 1988

Abstract: [1.1.1.1]- and [2.2.1.1]pagodanes **1/21** were oxidized in SbF_5/SO_2ClF at −78 °C via two-electron removal from the central cyclobutane ring to give the dications **9** and **24**, respectively. Dication **9** is also formed selectively by two-electron oxidation of a diene valence isomer of **1** (≡**19**) and by ionization of the Br_2 adduct of **1** (≡**18**). The unique dication **9** is stable at ambient temperature for hours, while the bishomologous **24** rearranges to a bisallylic dication, probably **28**, even at −78 °C. The tight structural prerequisites for the stability of such dications are further substantiated by the observation that from several related cyclobutanoid cage compounds **29–34**, when exposed to the same oxidative conditions, no distinct dications could be observed. On the basis of ^{1}H and ^{13}C NMR chemical shift criteria, supported by pertinent SCF-MO calculations, the dications obtained are considered as novel four-center/two-electron delocalized bishomoaromatic species, which resemble two-electron Woodward-Hoffmann transition states and owe their unprecedented character to their specific rigid framework. The reliability of the calculations in handling cage molecules of this type and size is evaluated in a comparison with structural data provided by single-crystal X-ray structure determinations for [1.1.1.1]- and [2.2.1.1]pagodanes **1/21** and dimethoxy product **16** obtained from quenching experiments with methanol.

The synthesis of the pentagonal dodecahedrane with its 20 equivalent methine units and 30 all-*cis,syn*-C-C ring junctions proved a formidable challenge. Although this undecacyclic, spherical skeleton is only slightly strained and thermodynamically excels as the "stabilomer"[2] of its class, complications en route are unavoidable due to increasing nonbonded, transannular interactions within intermediate stages. After early, unsuccessful attempts to overcome these obstacles by either thermodynamically controlled isomerization of selected precursors, convergent assembly of two fragments, or by stepwise constructions,[3] Paquette and co-workers ultimately succeeded in a "tour de force" multistep reaction sequence leading to the parent dodecahedrane and a series of derivatives.[3,4]

Profiting from earlier photochemical work,[5] the Freiburg group has developed and recently detailed[6] a synthetic strategy for the undecacyclic "pagodanes" A, allowing broad structural modifi-

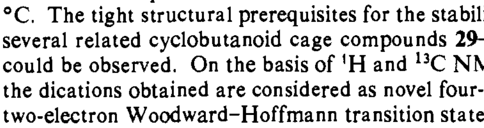

A B

cation (X, Y) as well as high product yields, as promising precursors for a class of variously modified dodecahedranes B.[7] Specifically, the $C_{20}H_{20}$ [1.1.1.1]pagodane **1** (≡A, X = Y = CH_2) exhibits very favorable structural and thermodynamic relationships with the parent dodecahedrane **3**.[8] Indeed, so far somewhat

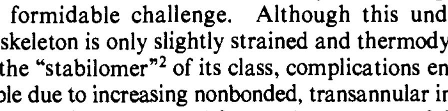

$C_{20}H_{20}$		$C_{20}H_{20}$
1	2	3
ΔH_f° = 64.4	(kcal/mol)	ΔH_f° = 22.2
E_{str} = 115.0	(MM2[5])	E_{str} = 68.9

limited success was achieved to convert pagodane into dodecahedrane along two strategic lines: by catalytic, thermodynamically controlled isomerization[9] and through a stepwise procedure via dibromide **18** and diene **19** as intermediates.[10] The initially planned short path by isomerization via carbocations **2**, making use of strong protic acids (e.g., triflic acid in dichloromethane), had only led to untractable material.[11] It has to be realized that with increasing size of the carbon skeleton the probability for competitive, irreversible pathways is steeply increasing. Recourse to superacid media, a methodology established for the efficient rearrangement of many hydrocarbons,[12] again did not furnish the target compound **3**. There was, however, an unexpected reward: pagodane **1**, instead of being isomerized to **3**, was cleanly oxidized by SbF_5-containing superacids to give a unique, theoretically intriguing bishomoaromatic dication.[13]

In this paper we report the full experimental and theoretical outcome of our joint investigation. We have extended this study to alternative precursors for this 2π-aromatic system (dibromide

† University of Southern California.
‡ Institut für Organische Chemie und Biochemie.

(1) Considered at University of Southern California as: Stable Carbocations, 273. Part 272. Olah, G. A.; Stephenson, M.; Shih, J. G.; Krishnamurthy, V. V.; Prakash, G. K. S. *J. Fluorine Chem.* **1988**, *40*, 319.
(2) Godleski, S. A.; Schleyer, P. v. R.; Osawa, E.; Wipke, W. T. *Prog. Phys. Org. Chem.* **1981**, *13*, 63. Iizuka, T.; Imai, M.; Tanaka, N.; Kan, T.; Osawa, E. *Chem. Abstr.* **1982**, *97*, 126567m.
(3) Reviews: Eaton, P. E. *Tetrahedron* **1979**, *35*, 2189–2223. Paquette, L. A.; Doherty, A. M. *Polyquinane Chemistry, Reactivity and Structure: Concepts in Organic Chemistry*; Springer Verlag: Berlin, 1987; Vol. 26.
(4) Paquette, L. A.; Ternansky, R. J.; Balogh, D. W.; Kentgen, G. *J. Am. Chem. Soc.* **1983**, *105*, 5446–5450. Paquette, L. A.; Weber, J. C.; Kobayashi, T. *J. Am. Chem. Soc.* **1988**, *110*, 1303–1304.
(5) Prinzbach, H.; Sedelmeier, G.; Krüger, C.; Goddard, R.; Martin, H.-D.; Gleiter, R. *Angew. Chem., Int. Ed. Engl.* **1978**, *17*, 271–273. Sedelmeier, G.; Fessner, W.-D.; Grund, C.; Spurr, P. R.; Fritz, H.; Prinzbach, H. *Tetrahedron Lett.* **1986**, *27*, 1277–1280. Melder, J.-P.; Wahl, F.; Fritz, H.; Prinzbach, H. *Chimia* **1987**, *41*, 426–428. See also ref 20 and 34.
(6) Fessner, W.-D.; Sedelmeier, G.; Spurr, P. R.; Rihs, G.; Prinzbach, H. *J. Am. Chem. Soc.* **1987**, *109*, 4626–4642.
(7) Prinzbach, H.; Fessner, W.-D. In *Organic Synthesis: Modern Trends*; Chizhov, O., Ed.; Blackwell Scientific: Oxford, 1987; pp 23–42.
(8) Fessner, W.-D.; Murty, B. A. R. C.; Prinzbach, H. *Angew. Chem., Int. Ed. Engl.* **1987**, *26*, 451–452.
(9) Fessner, W.-D.; Murty, B. A. R. C.; Wörth, J.; Hunkler, D.; Fritz, H.; Prinzbach, H.; Roth, W. R.; Schleyer, P. v. R.; McEwen, A. B.; Maier, W. F. *Angew. Chem., Int. Ed. Engl.* **1987**, *26*, 452–453.
(10) Spurr, P. R.; Murty, B. A. R. C.; Fessner, W.-D.; Fritz, H.; Prinzbach, H. *Angew. Chem., Int. Ed. Engl.* **1987**, *26*, 455–456.
(11) Fessner, W.-D. Ph.D. Dissertation, Universität Freiburg, 1986.
(12) Olah, G. A.; Olah, J. A. *Synthesis* **1973**, 488. Olah, G. A.; Farooq, O. *J. Org. Chem.* **1986**, *51*, 5410–5413, and references cited therein. Olah, G. A.; Stephenson, M.; Prakash, G. K. S., unpublished results.
(13) Preliminary communication: Prakash, G. K. S.; Krishnamurthy, V. V.; Herges, R.; Bau, R.; Yuan, H.; Olah, G. A.; Fessner, W.-D.; Prinzbach, H. *J. Am. Chem. Soc.* **1986**, *108*, 836–838.

0002-7863/88/1510-7764$01.50/0

18 and diene **19**[10]), to the bishomologous [2.2.1.1]pagodane **21**[11] and several cyclobutanoid polycycles **29–34**, the dications of which should be less stabilized by their respective frameworks. These studies also provide a better insight into the structural prerequisites for observable dications of cage hydrocarbons of this type.

Results and Discussion

The oxidative ionizations were carried out in SbF_5/SO_2ClF or $FSO_3H/SbF_5/SO_2ClF$ at −78 °C (dry ice/acetone) or −130 °C (liquid nitrogen/pentane slush). The ^1H and ^{13}C NMR spectra were recorded at 200 and 50 MHz, respectively, over a temperature range of −130 to 0 °C. Assignments for ^1H NMR signals are based on selective homonuclear decoupling experiments, for ^{13}C NMR signals on their multiplicity and relative intensity or by comparison with values of closely related cations.

[1.1.1.1]Pagodane 1. When 20 mg of **1** was dissolved in 1.5 mL of SO_2ClF containing a 5-fold excess of freshly distilled SbF_5 at −78 °C, the solution became instantaneously yellow. the proton spectrum recorded immediately consisted of complex broad signals in the aliphatic region, indicating the presence of paramagnetic radical cations, presumably **5** or **6**.[14] After ca. 3 h of standing

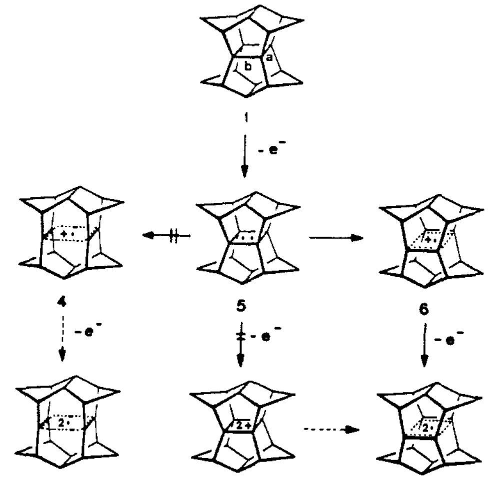

at the same temperature, the proton and carbon spectra had simplified to the 4-line pattern represented in Figure 1. No noticeable change was caused upon raising the temperature; in fact, the ion solution was found to be stable even at ambient temperature for several hours. As can be judged by the number of signals and their relative intensities, the newly formed species must have retained the D_{2h} symmetry of the parent system **1** with no change in the composition $C_{20}H_{20}$. The extent of deshielding in both spectra indicates the product to be ionic as a consequence of the removal of two electrons with both the positive charges being mainly located at the carbon atoms of the central cyclobutane ring.

On first sight, the three nonclassical dications **7–9** as well as the averaged structure of several classical dications **10–15** were considered as potential candidates. Further information was

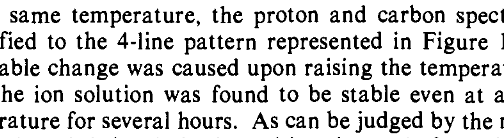

10 11 12

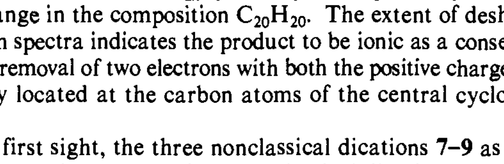

13 14 15

(14) Prinzbach, H.; Murty, B. A. R. C.; Fessner, W.-D.; Mortensen, J.; Heinze, J.; Gescheidt, G.; Gerson, F. *Angew. Chem., Int. Ed. Engl.* **1987**, *26*, 457–458.

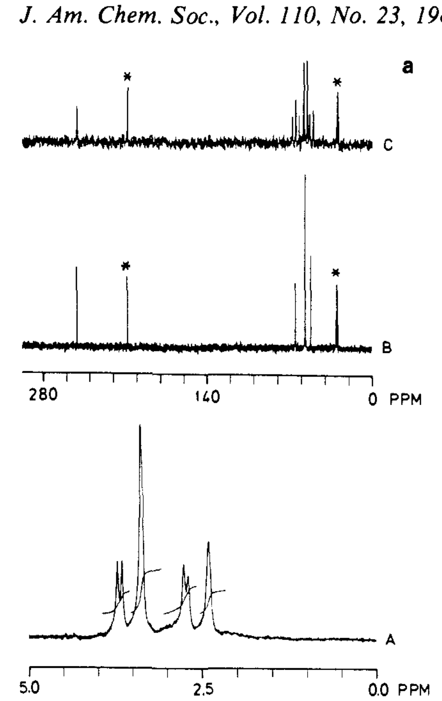

b

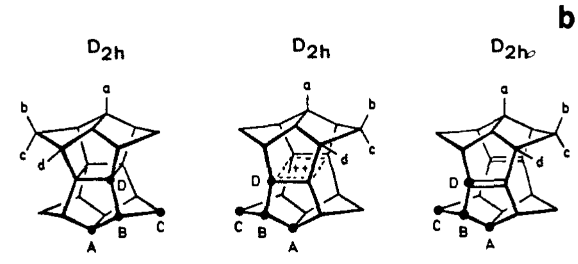

1 9 19

	1	Δ	9	Δ	19
a	2.60	+0.21	2.39	+0.89	3.28
b	1.56 (10.0)	−1.16	2.72 (13.2)	−1.40	1.32 (13.0)
c	1.60 (10.0)	−2.08	3.68 (13.2)	−0.77	2.91 (13.0)
d	2.24	−1.13	3.37	−0.28	3.09
A	59.6 (141)	+ 7.3	52.3 (152.8)	+9.8	62.1 (137)
B	42.7 (139)	− 14.5	57.2 (148.0)	−10.2	47.0 (136)
C	41.9 (130)	− 23.4	65.3 (141.9)	−32.6	32.7 (125)
D	62.9	−188.1	251.0	−95.6	155.4

Figure 1. a: (A) 200-MHz ^1H NMR spectrum of pagodane dication in SbF_5/SO_2ClF solution at −80 °C; (B)-50 MHz proton-decoupled ^{13}C NMR spectrum; (C) proton-coupled spectrum (* peaks due to lock solvent acetone-d_6). b: comparison of $^1H/^{13}C$ NMR data with those of **1** and **19**.

acquired by quenching experiments. After the ion solution was added to a mixture of methanol and sodium bicarbonate at −78 °C and the usual workup, a colorless solid was isolated that consisted of a single monomeric component (≥70% by ^{13}C NMR) and polymers. After repeated crystallizations from pentane, this compound was isolated (≥60%) as a crystalline material of mp 60 °C. Its $C_{22}H_{26}O_2$ composition ($C_{20}H_{20}$ + $2OCH_3$) was determined by mass spectrometry [*m/e* 322 (1.4, M^+), 292 (22.9),

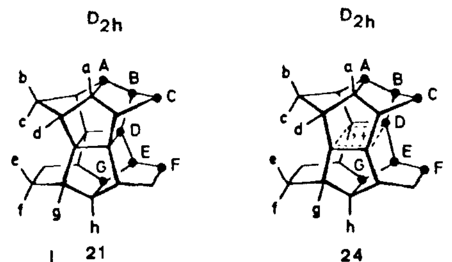

	21		24
a	2.69	+0.29	2.40
b	1.63	-0.97	2.60
c	1.53	-1.73	3.26
d	2.15	-0.94	3.09
e	1.56	+0.18	1.38
f	1.40	+0.02	1.38
g	1.61	-1.19	2.80
h	2.27	+0.64	1.63
A	59.8	+5.2	54.6
B	43.5	-14.8	58.3
C	40.9	-21.7	62.6
D	57.5	-177.7	235.2
E	34.0	-19.3	53.3
F	18.3	+7.8	10.5
G	48.5	+11.7	36.8

Figure 2. Comparison of $^1H/^{13}C$ NMR data of dication **24** with that of progenitor **21**.

291 (100, $M^+ - OCH_3$)] and its structure formulated as the C_{2v} symmetrical decacycle **16** on the basis of the NMR spectra. A

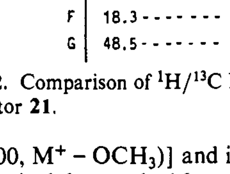

16

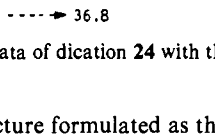

17

16: ^{1}H NMR ($CDCl_3$) δ 3.14 (s, 2 OCH_3), 2.62 (br s, 3-, 5-, 13-, 15-H), 2.54 (d, 4s-, 14s-H, J = 13.6 Hz), 2.38 (br s, 6-, 7-, 16-, 17-H + 8-, 10-, 18-, 20-H),* 1.79 (d, 9s-, 19s-H, J = 11.2 Hz), 1.39 (d, 4a-, 14a-H, J = 13.6 Hz); *(pyridine-d_5) δ 2.86 (m, 6-, 7-, 16-, 17-H), 2.88 (s, 8-, 10-, 18-, 20-H); ^{13}C NMR ($CDCl_3$) δ 101.5 (s, C-2, -12), 75.2 (s, C-1, -11), 58.8 (d, C-6, -7, -16, -17), 49.5 (q, OCH_3), 42.8 (d, C-8, -10, -18, -20), 41.7 (C-3, -5, -13, -15), 35.7 (dd, C-9, -19), 33.0 (dd, C-4, -14).

characteristic feature for this decacyclic skeleton, resembling that of dibromide **18** and excluding specifically the regioisomer **17**, is the presence of two types of methylene groups causing two AB patterns with J_{AB} = 11.2 Hz on the intact and J_{AB} = 13.6 Hz on the inverted (opened) site. An X-ray structure analysis, as shown in Figure 8, ultimately procured our assignment of the overall retained integrity of the basic skeleton and provided structural details which were helpful in the assessment of the various calculations (Table III). Earlier efforts on the X-ray structure determination of dibromide **18** or the parent $C_{20}H_{22}$ secopagodane[8] had failed due to disorder phenomena.[11,15]

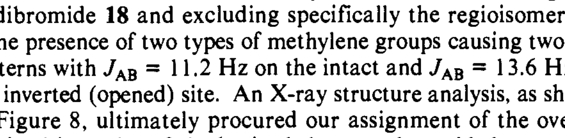

18 19 20

Consequently, it was not surprising that in continued work we were also successful in obtaining the same dicationic species from different precursors. Under the same ionizing conditions employed for pagodane **1**, ionization of dibromide **18** and oxidation of diene **19**, which had become available recently (in contrast, the diene isomer **20** remains still unknown),[10] neatly produced the same dication.

The "closed" dication **8** (the "real pagodane dication") or the "open" dication **7** (scission of bonds b) can safely be excluded as possible structures on the basis of the following facts: (i) the high tendency of cyclobutane radical cations (e.g., **5**) toward "symmetry-allowed" ring opening,[16] (ii) the identity of dications obtained from structurally differing precursors **1**, **18**, and **19**, and (iii) ^{13}C NMR chemical shift analysis.[17] As the NMR spectra shown in Figure 1 were found to be temperature independent down to -130 °C, it must be presumed that the D_{2h} symmetry of the ionic species is not the result of a rapid equilibration process, but rather due to the static dication **9**. Otherwise, the assumption would have to be made that the apparent symmetry is the result of very rapid equilibration processes ($E_a \leq 3$ kcal/mol) between degenerate dications of type **10–15**. Inasmuch as such an assumption can be dismissed on the basis of ^{13}C NMR chemical shift analysis[17] and subsequent arguments (vide infra), structure **9** becomes more probable, which implies the scission of bonds a in **1**. In fact, there is ample experimental and computational evidence for such a preference: (i) The relative lengths of the cyclobutane bonds in **1** as calculated by different methods[6,11] and measured by X-ray analysis (Figure 7 and Table III) indicate a weakening of bonds a; (ii) additions to pagodane, e.g., bromination to **18**, occur exclusively under opening of bonds a;[8,10] (iii) indications of hyperstability[18] for diene **19** and derivatives[10] demonstrate the favorable geometrical situation, especially when compared to the hypothetical, highly strained regioisomeric diene **20**;[8] and (iv) the homoconjugation of $\beta \approx 2$ eV for the bissecododecahedradiene **19**, as determined by PE spectroscopy,[19] which is basis for a ready and efficient [$\pi_2 + \pi_2$]-photocycloaddition,[20] provides proof of the optimal conditions for interactions between the perfectly collinear oriented π-orbitals, a situation that exactly is postulated in dication **9**.

[2.2.1.1]Pagodane 21. Increasing the length of the Y-bridges in pagodanes A from methylene as in **1** to ethylene as in **21** reduces the strain imposed on the "lateral" bonds a of the central four-membered ring. This becomes evident from calculations that predict a reduced bond length difference between bonds a and b (C1–C2 and C1–C11 in Table V, C1–C2 and C1–C13 in Table VII, respectively). The structural parameters of **21** (Figure 9 and Table VII), determined by X-ray analysis to amount to respective

(15) Pinkos, R. Diplomarbeit, Universität Freiburg, 1986. Cf.: Ermer, O. *Angew. Chem., Int. Ed. Engl.* **1983**, *22*, 246–247.

(16) Hammerich, O.; Parker, V. D. *Adv. Phys. Org. Chem.* **1984**, *20*, 55–189, 115ff. Haselbach, E.; Bally, T.; Lanyiova, Z.; Baertschi, P. *Helv. Chim. Acta* **1979**, *62*, 583–592. Roth, H.-D.; Schilling, M. L. M.; Mukai, T.; Miyashi, T. *Tetrahedron Lett.* **1983**, *24*, 5815–5818. Roth, H.-D. *Acc. Chem. Res.* **1987**, *20*, 343–350.

(17) One reviewer, who graciously identified himself as Prof. Paul v. R. Schleyer, suggested that the ^{13}C NMR chemical shift values for the observed dication species are more in favor of a rapidly equilibrating pair of classical dications **13–13'**. For such an equilibrating system, however, an average of chemical shifts for a typical classical C^+ center (δ ca. 330) and an α-carbon (δ ca. 70) of around δ 200 is to be expected; the actual value of δ 251 indicates a higher degree of unsaturation, as is realized in **9**. The expected range for typical carbenium ions by ^{13}C NMR chemical shift additivity analysis (Schleyer, P. v. R.; Lenoir, D.; Mison, P.; Liang, G.; Prakash, G. K. S.; Olah, G. A. *J. Am. Chem. Soc.* **1980**, *102*, 683–691) amounts to around 350–400 ppm per unit of positive charge. Application of this scheme to the observed dication reveals a total ^{13}C NMR shift difference of 500 ppm per unit of positive charge relative to pagodane **1** (as reference for a σ-dication **8**) and a difference of 543 ppm relative to secopagodane i[8] (as reference for a classical

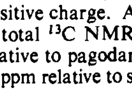

i

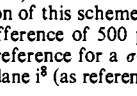

II

form **13**). The net chemical shift difference relative to bisseco-dodecahedrene II,[10] as a reference for π-dication **14**, amounts to 375 ppm per unit of positive charge. These results indeed support our views of the observed species being represented best by mesomeric forms **14–14'** ≡ **9**.

(18) Maier, W. F.; Schleyer, P. v. R. *J. Am. Chem. Soc.* **1981**, *103*, 1891–1900. McEwen, A. B.; Schleyer, P. v. R. *Ibid.* **1986**, *108*, 3951–3960.

(19) Hasenrück, K.; Mayer, B.; Martin, H.-D., private communication.

(20) Murty, B. A. R. C.; Spurr, P. R.; Pinkos, R.; Grund, C.; Fessner, W.-D.; Hunkler, D.; Fritz, H.; Roth, W. R.; Prinzbach, H. *Chimia* **1987**, *41*, 32–35.

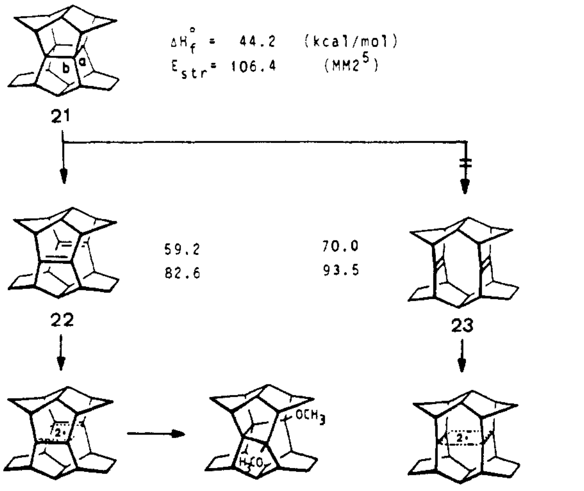

averaged lengths of 1.560 and 1.549 Å, are in good agreement with this argument. Nevertheless, regioselective scission of bonds a to give diene **22** should still be thermodynamically preferred.[11,21] because of the bicyclo[2.2.2]octane-type partial structure in **21**, secondary transformations of dication **24** (**26**) by hydride shift or proton loss, i.e., anti-Bredt olefin formation, become more likely than in **9**.[18]

Upon dissolution of **21** in the superacid medium at −78 °C, both ^{1}H and ^{13}C NMR monitoring revealed spontaneous line broadening, as was the case for **1**. After several hours, well-resolved 8-line proton and carbon spectra emerged. Spectral comparison strongly suggested formation of dication **24** as opposed to regioisomer **26**. The chemical shift differences compiled in Figure 2, particularly those for the analogous [1.1] subunit, closely match the values determined for **9** (Figure 1). The somewhat reduced shift effects can be interpreted to reflect the slightly increased molecular dimensions in **24** with a resulting diminished transannular resonance as opposed to **9**.

Even at −78 °C, however, and increasingly at higher temperature, additional signals were recorded. On warming to 0 °C, the original lines had completely disappeared. when the solution was kept at −20 °C, a major species (>70%) could be distinguished to which the structure of the C_2 symmetrical bisallylic dication **28** is tentatively assigned. The assumption of anti-Bredt diene

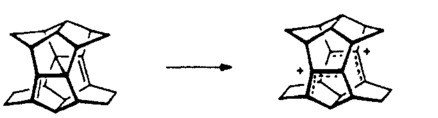

27 28

27 or an equivalent thereof as an intermediate precursor seems to be reasonable. Increasing likelihood for competing pathways, or the presence of more than one ionic product, is attested to by quenching experiments on a freshly prepared sample of **24** with methanol at −78 °C: GC/MS analysis confirmed a compound of composition $C_{24}H_{30}O_2$ ($C_{22}H_{24}$ + $2OCH_3$) in accord with the presumed **25** as the principal component (>60%) among a rather complex mixture of additional products.

Cyclobutanoid Cage Compounds 29–34. The behavior of the bishomologous dication **24** already indicates a delicate influence of the molecular geometry embodying the special bonding arrangement upon stability. From a study of the series of polycycles **29**–**34**[22] that incorporate fixed, planar cyclobutane subunits into more or less strained cages, further insight was expected into requirements for the stability of such bishomoaromatic dications.

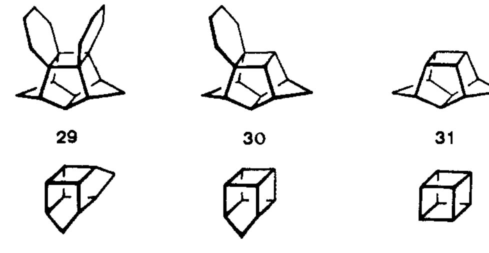

29 30 31
32 33 34

Under the variously modified conditions employed (SbF_5 or FSO_3H/SbF_5 in SO_2ClF at −78 or −130 °C), however, for none of these compounds could a stable, discernable ionic product of a type analogous to **9** and **24** be observed. Probably, after one-electron oxidation, ring opening to more flexible, kinetically less-protected polycyclic structures occurs which may then decompose or polymerize under the reaction conditions.

Computational Analysis

The dications **9** and **24** are considered as the first representatives of a novel class of 2π-"aromatic" pericyclic systems, topologically equivalent to the transition state for the Woodward–Hoffmann "allowed" cycloaddition **35** of ethylene to ethylene dication.[23] In

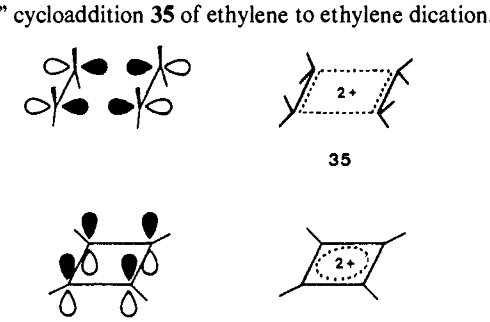

35

36

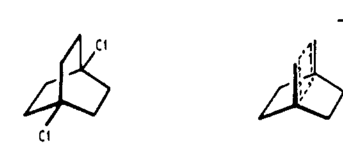

37

contrast to the well-studied cyclobutadiene dication **36** with conventional π-type delocalization,[24,25] in **35** (**9**/**24**) delocalization occurs among the orbitals in the plane of the (bishomo)conjugated system. A precedent case of this type, the assumed 1,4-bicyclo[2.2.2]octanediyl dication for which one canonical structure **37** is shown,[24] was found in a recent reinvestigation to be the monocation–monodonor acceptor complex.[26] Nevertheless, the theoretical arguments[24] put forward in the context with **37** are still valid for **9** and **24**.

The bonding situation of the parent C_4H_8 dication **35** was analyzed by ab initio STO-3G theory.[27] The pagodane envi-

(21) A limiting difference in reactivity between the pagodanes **1** and **21** was noted during attempts to prepare dienes **22** or **23** in the same fashion as diene **19** was obtained from **1**. Photobromination resulted in a complex mixture of bromides from which after chromatography the carbinols iii/iv

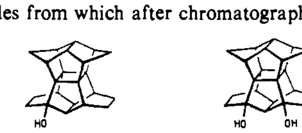

iii iv

were acquired as the main components (ca. 20% each). Prinzbach, H.; Melder, J.-P.; Pinkos, R.; Lutz, G., unpublished results.

(22) A sample of **34** was kindly provided by Prof. P. E. Eaton.

(23) Goldstein, M. J.; Hoffmann, R. *J. Am. Chem. Soc.* **1971**, *93*, 6193–6204.

(24) Olah, G. A.; Liang, G.; Schleyer, P. v. R.; Engler, E. M.; Dewar, M. J. S.; Bingham, R. C. *J. Am. Chem. Soc.* **1973**, *95*, 6829–6831. Prakash, G. K. S.; Rawdah, T. N.; Olah, G. A. *Angew. Chem., Int. Ed. Engl.* **1983**, *22*, 390–402. Childs, F. R.; McGlinchey, M. J.; Varadarajan, A. *J. Am. Chem. Soc.* **1984** *106*, 5974–5978.

(25) Cyclobutadiene dication appears to have a puckered ground-state structure: Krogh-Jespersen, K.; Schleyer, P. v. R.; Pople, J. A.; Cremer, D. *J. Am. Chem. Soc.* **1978**, *100*, 4301–4302. Hess, B. A., Jr.; Ewig, C. S.; Schaad, L. J. *J. Org. Chem.* **1985**, *50*, 5869–5871.

(26) de Meijere, A.; Schallner, O.; Weber, W.; Schleyer, P. v. R.; Prakash, G. K. S.; Olah, G. A. *J. Org. Chem.* **1985**, *50*, 5255–5257.

Scheme I. Calculated Relative Enthalpies of Formation (kcal/mol) for Pagodane Dication Isomers and Activation Barriers for Selected Interconversions (MNDO)[a]

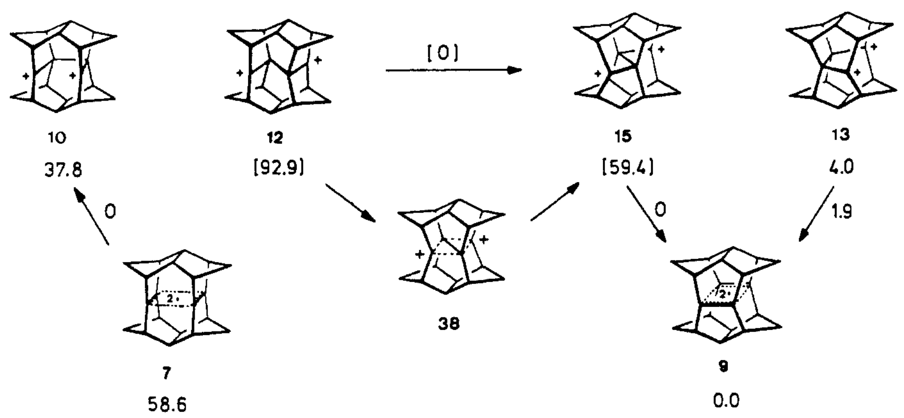

[a] Numbers in brackets refer to optimized structures with fixed values for α-(1.5 Å; **12**) and β-bonds (1.6 Å; **12** and **15**).

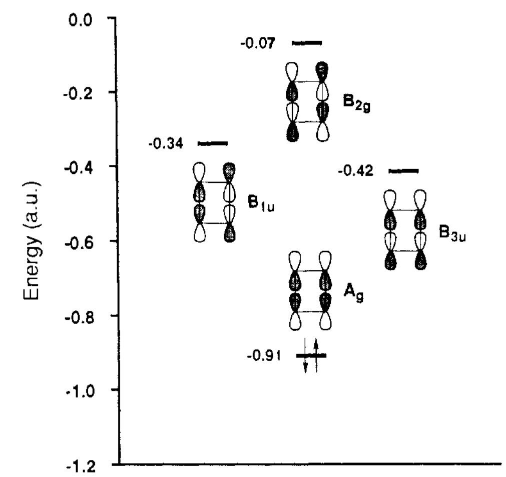

Figure 3. MO diagram of rectangular cyclobutane dication **35** (STO-3G).

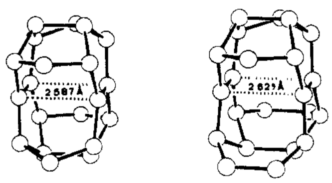

9 24

Figure 4. MNDO-optimized structures of dications **9** and **24**.

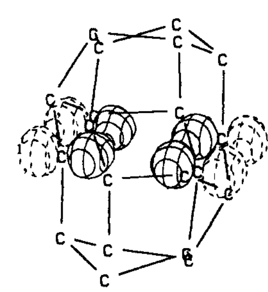

Figure 5. Jorgensen plot[31] of the highest occupied molecular orbital of **9**. The orbital size is scaled down for clarity.

ronment was simulated by a constraint of D_{2h} symmetry. The retangular minimum structure obtained is characterized by two sets of C–C bonds that differ pronouncedly in their nature. The length of the two shorter bonds with 1.447 Å suggests a considerable π-character with a bond order between a C—C single and a C=C double bond, whereas the other pair with 2.020 Å corresponds to a substantially elongated C—C single bond, implying a bond order of ~0.5. In the π-MO diagram of **35**, shown in Figure 3, the lowest bonding MO is occupied by two electrons and this rationalizes the profitable bonding interaction.

A detailed study of the pagodane dication **9** itself was restricted because of its size to semiempirical SCF-MO calculations.[28] The MNDO approximation was chosen because it had given a superior fit to the experimental X-ray data for this type of (uncharged) caged structures (see Tables III and V and Figure 10), on the assumption that results for the charged isomeric structures considered should be of comparable accuracy due to the rigidity of the cages.

An exploration of the energy potential surface (Scheme I) furnished three local minima corresponding to structures **9**, **10**, and **13**. The assumed nonclassical D_{2h} isomer **7** (bond distances 1.487 and 2.219 Å) collapses to **10** without activation when the imposed symmetry is reduced to C_{2v}, indicating it to be only a transition state for a degenerate isomerization of **10**. Geometries corresponding to the highly distorted classical C_{2h} isomers **12** and **15** could only be obtained when the bonds separating the cationic centers were frozen to constant values. Upon release of the α-bonds (1.5 Å) in **12**, the structure collapses to **15** through a process that resembles a dyotropic rearrangement (**38**).[29] Further liberation of the transannular β-bond (1.6 Å) in **15** leads to the minimum structure **9**, also without activation. According to MNDO, the classical dication **13** (transannular β-bond 1.724 Å) is 4.0 kcal/mol higher in energy than the experimentally favored **9** and separated from the latter by a barrier of only 1.9 kcal/mol. Although energetically close to the classical alternative **13**, dication **9** clearly represents the true energy minimum for this computational level. On the AM1 and MINDO/3 levels, equilibrium structure **9** also constitutes the (by far) most stable geometry, while a classical dication **13**, however, is no longer a local minimum.[30]

The rectangular D_{2h} structure of **9**, drawn in Figure 4, reveals a closer resemblance with the (calculated) geometry of diene **19**

(27) Binkley, J. S.; Pople, J. A.; Hehre, W. J. *J. Am. Chem. Soc.* **1980**, *102*, 939. Gordon, M. S.; Binkley, J. S.; Pople, J. A.; Pietro, W. J.; Hehre, W. J. *Ibid.* **1982**, *104*, 2797–2803. Binkley, J. S.; Whiteside, R. A.; Krishnan, R.; Seeger, R.; DeFrees, D. J.; Schlegel, H. R.; Topiol, S.; Kahn, L. R.; Pople, J. A. *QCPE* **1981**, *13*, 406. Van Kamper, P. N.; Smiths, G. F.; De Leeuw, F. A. M.; Altona, C. *QCPE* **1982**, *14*, 437.

(28) AM1: Dewar, M. J. S.; Zoebisch, E. G.; Healy, E. F.; Stewart, J. J. P. *J. Am. Chem. Soc.* **1985**, *107*, 3902–3909. MNDO: Dewar, M. J. S.; Thiel, W. *Ibid.* **1977**, *99*, 4899–4907. MINDO/3: Bingham, R. C.; Dewar, M. J. S.; Lo, D. H. *Ibid.* **1975**, *97*, 1285–1293. We are grateful to Prof. K. N. Houk for making the AMPAC program package available to us.

(29) Schleyer, P. v. R.; Kos, A. J., unpublished results and private communication. Fessner, W.-D.; Prinzbach, H., unpublished results. Details of these investigations will be published elsewhere.

(30) The parametrizations of AM1 and MINDO/3 are more in favor of nonclassical structures.[29] Cf. the absolute energy differences predicted for dications **39** and **40** in Figure 6.

(31) Cf.: Jorgensen, W. L.; Salem, L. *The Organic Chemist's Book of Orbitals*; Academic: New York, 1973.

39

40

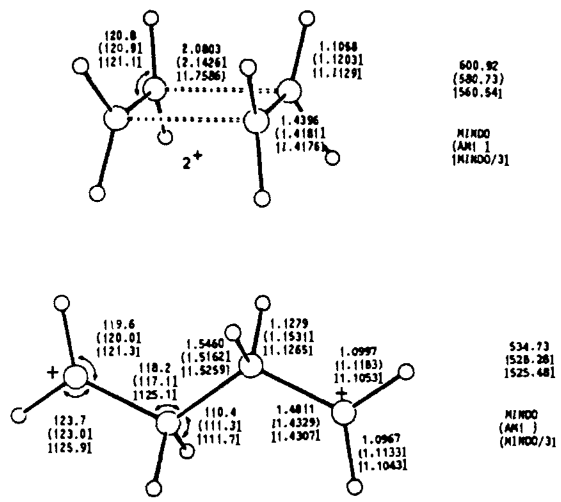

Figure 6. Calculated structures (Å, deg) and enthalpies (kcal/mol) of $(CH_2)_4$ dications **39** and **40** from MNDO, AM1 (parenthetical values), and MINDO/3 (in square brackets).

Table I. Comparison of Selected Structural Data of **9** with That of **1** and **19** (MNDO)

type	1	9	19
	Bond Lengths, Å		
1–2	1.614	2.587	2.842
1–11	1.570	1.461	1.376
1–5	1.547	1.511	1.523
	Bond/Torsional Angles, deg		
1–2–3	103.2	84.8	82.5
5–1–11–15	152.2	187.3	196.2

rather than with that of pagodane **1** (Table I) nor with diene **20**. This conclusion is corroborated experimentally in certain NMR features, e.g., the characteristic geminal coupling constant of 13.2 Hz (cf. data for **15**). Analogous to the findings for the parent **35** discussed above, the calculations on **9** indicate a long bond **a** distance of 2.587 Å, though appreciably shorter by ca. 0.25 Å relative to **19** and far below the van der Waals π/π-distance (ca. 3.4 Å). Again, this situation represents a bond order of roughly half a single bond, whereas for the bonds **b** with a value between those of **1** and **19** a bond order of ca. 1.5 is predicted. The calculated in-phase π-combination of the highest occupied MO of **7**, responsible for the bishomoaromatic stabilization, is visualized in Figure 5. The pyramidalization postulated[10] for the olefinic carbons in **19** is largely diminished in the dication **9** (Table I). Most remarkably, the major part of the two positive charges (ca. 1.5 units) is predicted to be delocalized into the molecular periphery, i.e., into the C–H bonds.

Similar features are predicted for the bishomologous dication **24** (Figure 4). Due to the larger bridges in the "lower" molecular half, a slightly enhanced internal diameter (2.621 Å) in association with a minimal deviation of the π-orbitals from collinearity (ω ca. 173°) are reasons for a reduced transannular overlap.

Additional information about the absolute order of stability of dications of type **35** was evaluated by calculations on a family of tetramethylene dications considering different cyclic and linear structures of varying symmetry.[29] With different semiempirical approximations, the rectangular "aromatic" structure **39** represents the energy minimum for cyclic cases and the C_{2h} trans structure **40**, with the greatest possible distance between the cationic centers, the (global) energy minimum for the linear series (Figure 6). Similar conclusions were reached by Schleyer et al.[29] on the basis of ab initio calculations.

The huge energy gap between cyclic (**39**) and linear (**40**) geometries, appreciably diminished but not vanishing on higher ab initio levels,[29] stresses the importance of special, rigid frameworks for the formation and kinetic protection of dications of these types, as experimentally manifested in the substrate series **1**, **21**, and **29–34**.

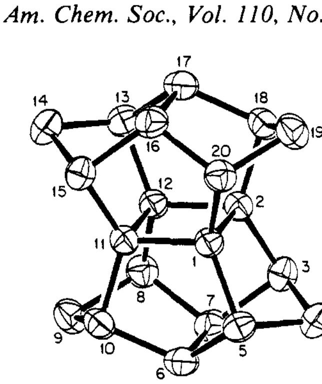

Figure 7. ORTEP plot of [1.1.1.1]pagodane **1**, with thermal ellipsoids at the 50% probability level. Atoms are labeled according to the IUPAC nomenclature. Hydrogen atoms are omitted for clarity.

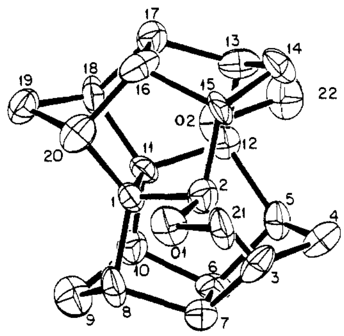

Figure 8. ORTEP plot of dication quenching product **16** (for further details, see Figure 7).

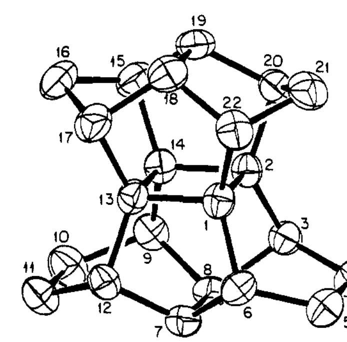

Figure 9. ORTEP plot of [2.2.1.1]pagodane **21** (for further details, see Figure 7).

Conclusion and Remarks

An accepted experimental criterium for the qualification of **9** and **24** as "bishomoaromatic" 2π-species (Figure 3) would be the detection of a ring current.[32] The similarity of the cyclobutanoid ^{13}C shift for **9**/**24** (δ 251.0 and 235.2) and tetramethylcyclobutadiene dication (δ 209.7) is remarkable, though not necessarily convincing because of the difference in bonding. With due reservation, the following ^1H and ^{13}C NMR details are offered as indicators for the existence of such a current: (i) The ^1H and ^{13}C signals for the a/A nuclei in **9** (Figure 1), centrally located above the 2π-plane, are substantially shifted to higher field with respect to **19** (**1**) [$\Delta\delta$ = 0.89(0.21)/9.5(7.3) ppm]; (ii) similar high-field shifts are found for the respective a/A signals of dication **24** with respect to **21** ($\Delta\delta$ = 0.29/5.3 ppm) and about twice as large ($\Delta\delta$ = 0.64/11.7 ppm) for the corresponding signals in the bishomologous [2.2] part.

We fully realize that suggesting "aromatic" nature for **9** and **24** by necessity is somewhat arbitrary. However, the obtained experimental results (unexpected stability, NMR chemical shift analysis) and calculational data justify such a suggestion.

The relatively long-lasting broadening of the NMR signals accompanying the dissolution of **1** or **21** and **19** in the oxidizing

(32) Olah, G. A.; Staral, J. S. *J. Am. Chem. Soc.* **1976**, *98*, 6290–6304.

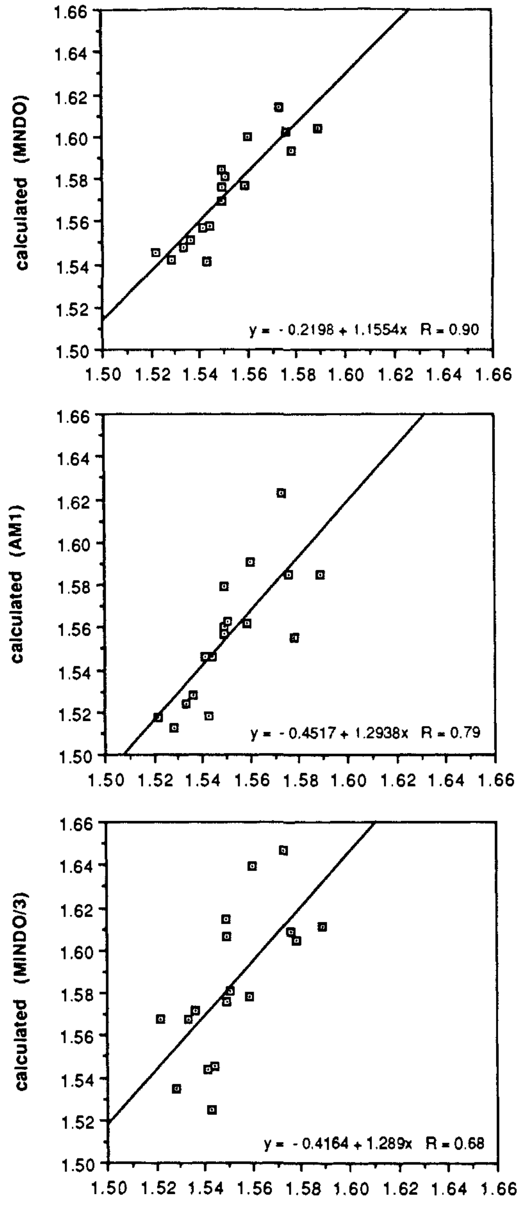

Figure 10. Performance of semiempirical SCF-MO methods: comparison of calculated structure data (MNDO, AM1, MINDO/3) with experimentally determined bond distances (Å) for hydrocarbons **1** and **21** (least-squares linear regression analysis).

medium suggested the initial formation of relatively long-lived, unusually stable radical cations. Recent voltammetric and ESR studies have unraveled the individual steps.[14] Thus, the oxidation of pagodane **1** to **9** follows an ECE course (appearance voltage +1.2 V vs Ag/AgCl) via the "open" radical cation **6**, which is also directly obtained from diene **19** (+0.66 V). In the ESR study, the deeply colored radical cations of **1** and **21**, of fully delocalized nature (e.g., **6**), proved to be unusually persistent, exhibiting the same structure–stability relationship as observed for the dications. Again, for the "molecular moieties", e.g., **29** under neither electrochemical nor ESR conditions were radicals (cations) detected. Our hopes, that the rigid framework of **1** and **19** or **21** might allow the experimental distinction between valence isomeric dications (e.g., closed **8** and open **9**) in the gas phase by charge-stripping mass spectrometry, were not fulfilled.[33] Again, the same dication was observed starting from **1** and **19**. Under these conditions, however, even for simpler structures like **31** the characteristic dication signals were recorded.

(33) Drewello, T.; Fessner, W.-D.; Kos, A. J.; Lebrilla, S. B.; Prinzbach, H.; Schleyer, P. v. R.; Schwarz, H. *Chem. Ber.* **1988**, *121*, 187–189.

Table II. Summary of Crystal Data and Refinement Results for **1**, **16**, and **21**

	1	16	21
crystal dimensions, mm	0.65 × 0.65 × 0.20	0.23 × 0.18 × 0.18	0.20 × 0.16 × 0.16
space group	$P\bar{1}$	*Fdd*2	$P2_1/c$
molecules/unit cell	1	16	4
a, Å	7.304 (5)	12.665 (1)	6.512 (4)
b, Å	8.182 (4)	63.343 (54)	14.976 (10)
c, Å	6.336 (3)	8.581 (11)	14.853 (14)
α, deg	105.50 (4)	90.00	90.00
β, deg	112.07 (5)	90.00	91.62 (6)
γ, deg	64.97 (5)	90.00	90.00
V, Å³	315.3 (4)	6884 (12)	1448 (2)
d_{calcd}, g cm^{-3}	1.37	1.24	1.32
data collectn wavelength, Å	0.71069	0.71069	0.71069
sin θ/λ limit, Å^{-1}	0.650	0.538	0.538
total no. of unique data	1664	2173	1909
no. of obsd data	1387	1220	1217
N (parameters)	91	231	199
final agreement factors			
R(*F*)	0.055	0.066	0.049
$R_w(F)$	0.078	0.085	0.055

The outcome of the calculations[29] entailed the question of what impact a symmetry enforcement toward D_{4h} (i.e., equivalence of cyclobutane bonds) would have upon respective C_4 dications. Unfortunately, our preparative efforts toward isopagodane **41**,[7,34]

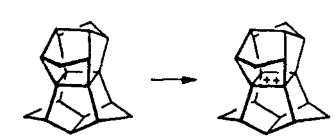

41 **42**

the precursor for a dication **42** approaching this symmetry state, have been thwarted so far by our inability to effect the crucial photochemical step[20] in a synthetic scheme patterned after that worked out for **1**.[6,35]

Ongoing studies in this context are also focused upon the synthesis of the linking [2.1.1.1]- (**43**) and the [1.1.0.0]- and [0.0.0.0]pagodanes **44** and **45** (a "2-fold pentaprismane"[38]) as precursors for their respective cation radicals and dications as well as for their valence isomeric dienes. Unusual properties are intrinsically bound to such unusual molecular entities.

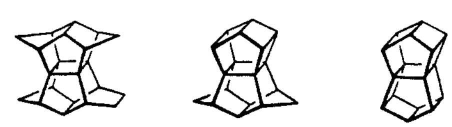

43 **44** **45**

Experimental Section

¹H and ¹³C NMR spectra were obtained on either a Varian Associates Model XL-200 or VXR-200 spectrometers equipped with broad-band

(34) Sedelmeier, G.; Fessner, W.-D.; Pinkos, R.; Grund, C.; Murty, B. A. R. C.; Hunkler, D.; Rihs, G.; Fritz, H.; Krüger, C.; Prinzbach, H. *Chem. Ber.* **1986**, *119*, 3442–3472.

(35) The $C_{16}H_{24}$ polycycle v, the [3.3.3.3]tetraannulane[36] core of pagodane **1** and isopagodane **40**, has recently been synthesized.[37] Its potential D_{4d} symmetrical dication vi lacks, however, "anti-Bredt protection" and the skeletal

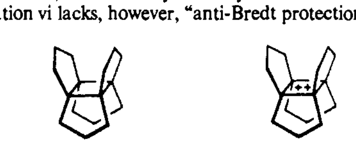

v vi

rigidity that this study shows are prerequisites for significant stability.

(36) Marshall, J. A.; Peterson, J. C.; Lebioda, L. J. *J. Am. Chem. Soc.* **1983**, *105*, 6515–6516.

(37) Fitjer, L.; Quabeck, U. *Angew. Chem., Int. Ed. Engl.* **1987**, *26*, 1023–1024.

(38) Eaton, P. E.; Or, Y. S.; Branca, S. J.; Shankar, B. K. R. *Tetrahedron* **1986**, *42*, 1621–1631.

Table III. Experimental and Calculated Bond Distances (Å) for **1**

type	exptl	exptl (av)	MNDO	AM1	MINDO/3
C1–C2 = C11–C12	1.573 (2)	1.573	1.614	1.623	1.647
C1–C5 = C12–C13	1.532 (2)	1.533	1.548	1.524	1.568
C1–C20 = C8–C12	1.536 (2)				
C2–C3 = C11–C15	1.530 (2)				
C2–C18 = C10–C11	1.534 (2)				
C1–C11 = C2–C12	1.549 (2)	1.549	1.569	1.557	1.606
C3–C4 = C14–C15	1.546 (2)	1.544	1.558	1.546	1.545
C4–C5 = C13–C14	1.540 (2)				
C8–C9 = C19–C20	1.543 (2)				
C9–C10 = C18–C19	1.547 (2)				
C3–C7 = C15–C16	1.561 (2)	1.559	1.577	1.562	1.578
C5–C6 = C13–C17	1.557 (2)				
C6–C10 = C17–C18	1.557 (2)				
C7–C8 = C16–C20	1.559 (2)				
C6–C7 = C16–C17	1.589 (2)	1.589	1.604	1.585	1.611
nonbonded distance					
C4–C19 = C9–C14	3.530 (2)		3.569	3.498	3.630

Table IV. Selected Bond Angles (deg) for **1**

type	angle
C2–C1–C5 = C11–C12–C13	103.6 (1)
C2–C1–C11 = C2–C12–C11	90.0 (1)
C2–C1–C20 = C8–C12–C11	103.5 (1)
C5–C1–C11 = C2–C12–C13	109.1 (1)
C5–C1–C20 = C8–C12–C13	132.6 (1)
C11–C1–C20 = C2–C12–C8	109.1 (1)
C1–C2–C3 = C12–C11–C15	103.7 (1)
C1–C2–C12 = C1–C11–C12	90.0 (1)
C1–C2–C18 = C10–C11–C12	103.6 (1)
C3–C2–C12 = C1–C11–C15	109.0 (1)
C3–C2–C18 = C10–C11–C15	132.5 (1)
C12–C2–C18 = C1–C11–C10	109.1 (1)
C2–C3–C4 = C11–C15–C14	103.8 (1)
C2–C3–C7 = C11–C15–C16	99.5 (1)
C4–C3–C7 = C14–C15–C16	102.6 (1)
C3–C4–C5 = C13–C14–C15	96.1 (1)
C1–C5–C4 = C1–C13–C14	104.0 (1)
C1–C5–C6 = C12–C13–C17	99.4 (1)
C4–C5–C6 = C14–C13–C17	103.2 (1)
C7–C6–C8 = C13–C17–C16	102.9 (1)
C7–C6–C10 = C16–C17–C18	103.0 (1)
C8–C6–C10 = C13–C17–C18	110.1 (1)
C3–C7–C6 = C15–C16–C17	103.2 (1)
C3–C7–C8 = C15–C16–C20	109.6 (1)
C7–C8–C9 = C16–C20–C19	102.7 (1)
C7–C8–C12 = C1–C20–C16	99.3 (1)
C9–C8–C12 = C1–C20–C19	104.4 (1)
C8–C9–C10 = C18–C19–C20	95.8 (1)
C6–C10–C9 = C17–C18–C19	102.8 (1)
C6–C10–C11 = C2–C18–C17	99.3 (1)
C9–C10–C11 = C2–C18–C19	104.3 (1)

variable-temperature probes. ^1H and ^{13}C NMR chemical shifts for cations are referenced to external capillary tetramethylsilane.

Pagodanes and derivatives **1**, **18**, **19**, and **21** were prepared as previously described.[6,10] Hydrocarbons **31**,[39] **32**,[40] and **33**[41] were synthesized according to literature procedures. A sample of cubane **34** was kindly provided by Prof. P. E. Eaton.

Compounds **29** and **30** were obtained by H_2–Pd/C-catalyzed saturation of previously described olefinic precursors:[6]

Octacyclo[12.5.1.0^{2,7}.0^{2,13}.0^{7,18}.0^{8,13}.0^{8,16}.0^{17,20}]eicosane (29): fine, colorless needles from ethanol; mp 188 °C; IR (KBr) 3005, 2915, 2845, 1455, 1440, 1280, 1240 cm^{-1}; ^1H NMR δ 2.25 (m, 17-, 20-H), 1.91, (m, 1-, 14-, 16-, 18-H), 1.84 (m, 3n-, 6n-, 9n-, 12n-H), 1.69 (dm, 15a-, 19a-H), 1.62 (dm, 15s-, 19s-H), 1.49–1.17 (overlapping m, 3x-, 6x-, 9x-, 12x- and 4-, 5-, 10-, 11-H); ^{13}C NMR δ 55.9 (C-1, -14, -16, -18), 51.8 (C-2, -7, -8, -13), 50.8 (C-17, -20), 39.8 (C-15, -19), 28.0 (C-3, -6, -9, -12), 23.3 (C-4, -5, -10, -11). Anal. Calcd for $C_{20}H_{26}$ (266.4): C, 90.16; H, 9.84. Found: C, 90.09; H, 9.88.

Heptacyclo[8.5.1.0^{2,9}.0^{3,8}.0^{3,14}.0^{8,12}.0^{11,15}]hexadecane (30). An analytical sample was obtained by bulb-to-bulb distillation: bp 120 °C (14 mm); IR (neat) 2940, 2930, 2855, 1450, 1285, 1240 cm^{-1}; ^1H NMR δ 2.36 (m, 1-, 2-, 9-, 10-H), 2.24 (m, 11-, 15-H), 1.87 (m, 12-, 14-H), 1.79–1.21 (overlapping m, 4-, 5-, 6-, 7-, 13-, 16-H); ^{13}C NMR δ 53.2 (d, 2 C), 52.8 (d, 2 C), 51.4 (C-3, -8), 46.6 (d, 2 C), 45.4 (d, 2 C), 41.4, 38.5 (C-13, -16), 28.1 (C-4, -7), 20.5 (C-5, -6). Anal. Calcd for $C_{16}H_{20}$ (212.3): C, 90.51; H, 9.49. Found: C, 90.39; H, 9.60.

Table V. Experimental and Calculated Bond Distances (Å) for **16**[a]

type	exptl	exptl (av)	MNDO	AM1	MINDO/3
C1–C2	1.547 (11)	1.527	1.598	1.562	1.619
C11–C12	1.506 (11)				
C1–C8	1.529 (11)	1.528	1.558	1.538	1.574
C1–C20	1.521 (11)				
C10–C11	1.529 (11)				
C11–C18	1.531 (11)				
C1–C11	1.598 (10)	1.598	1.653	1.610	1.711
C2–C3	1.556 (11)	1.553	1.585	1.548	1.586
C2–C15	1.522 (1)				
C5–C12	1.575 (11)				
C12–C13	1.560 (11)				
C3–C4	1.538 (12)	1.532	1.540	1.518	1.537
C4–C5	1.520 (12)				
C13–C14	1.532 (11)				
C14–C15	1.536 (12)				
C3–C7	1.553 (11)	1.570	1.575	1.560	1.579
C5–C6	1.548 (11)				
C13–C17	1.581 (11)				
C15–C16	1.596 (12)				
C6–C7	1.577 (12)	1.577	1.583	1.565	1.593
C16–C17	1.576 (12)				
C6–C10	1.569 (12)	1.578	1.576	1.563	1.578
C7–C8	1.583 (11)				
C16–C20	1.551 (12)				
C17–C18	1.607 (12)				
C8–C9	1.514 (11)	1.540	1.545	1.534	1.535
C9–C10	1.529 (12)				
C18–C19	1.549 (12)				
C19–C20	1.569 (12)				
O1–C2	1.466 (11)				
O–C21	1.421 (11)				
O2–C12	1.457 (11)				
O2–C22	1.440 (11)				
nonbonded distances					
C2–C12	3.036 (11)		3.169	3.029	3.161
C4–C14	3.421 (12)		3.510	3.439	3.581
C9–C19	3.117 (12)		3.126	3.062	3.159

[a] Calculated values for dihydroxy compound.

Preparation of Ions. SbF_5 and FSO_3H were freshly distilled before use. To the appropriate superacid dissolved in a 2-fold excessive amount of SO_2ClF or SO_2 at dry ice/acetone temperature (−78 °C) or pentane/liquid nitrogen slush (ca. −130 °C) was slowly added with vigorous stirring a cooled slurry or solution of the appropriate precursor in SO_2ClF or SO_2, resulting in an approximately 10–15% solution of the ion. The quenching experiments were carried out by pouring the ion solution into methanol/sodium bicarbonate slush at −78 °C. The resulting solution was brought to room temperature, extracted with dichloromethane, and washed with water. Evaporation gave the crude ether derivative which was further purified by recrystallization from hexane/ether and pentane (≥60% isolated yield of **16**).

Molecular Orbital Calculations. The reported calculations were performed with the programs provided in the MNDOC and AMPAC packages on UNIVAC 1100/82 and DEC VAX 11/780 computer systems, respectively. Unless otherwise stated, full geometry optimizations were performed assuming highest applicable point group symmetries. Reaction pathways were calculated by using the program-incorporated option at 0.1-Å steps.

As an assessment of the performance of semiempirical SCF–MO methods in this ballpark of cage structures, a comparison was made of the (averaged) experimental data with calculated values for hydrocarbons **1** and **21** (cf. Tables III and VII). The plots in Figure 10 demonstrate that the most recent parametrization of AM1 gives rather scattered data, while with MNDO satisfactory geometries are obtained. In the linear regression analysis for the latter with a good correlation of $R = 0.9$, the

(39) Bruck, P.; Thompson, D.; Winstein, S. *Chem. Ind. (London)* **1960**, 405–406. Soloway, S. B.; Damiana, A. M.; Sims, J. W.; Bluestone, H.; Lidov, R. E. *J. Am. Chem. Soc.* **1960**, *82*, 5377–5385.

(40) Schenck, G. O.; Steinmetz, R. *Chem. Ber.* **1963**, *96*, 520–525.

(41) Dunn, G. L.; DiPasquo, V. J.; Hoover, J. R. E. *Tetrahedron Lett.* **1966**, 3737–3742. Dauben, W. G.; Whalen, D. L. *Ibid.* **1966**, 3743–3750.

Table VI. Selected Bond Angles (deg) for **16**

type	angle	type	angle
C2–C1–C8	103.8 (6)	C1–C11–C12	118.3 (6)
C2–C1–C11	117.9 (6)	C1–C11–C18	102.0 (6)
C2–C1–C20	103.0 (6)	C10–C11–C12	104.2 (6)
C8–C1–C11	102.6 (6)	C10–C11–C18	126.8 (6)
C8–C1–C20	127.5 (6)	C12–C11–C18	104.2 (6)
C20–C1–C11	103.3 (6)	C5–C12–C11	104.3 (6)
C1–C2–C3	103.8 (6)	C5–C12–C13	127.8 (6)
C1–C2–C15	104.3 (6)	C5–C12–O2	106.3 (6)
C1–C2–O1	102.4 (6)	C11–C12–C13	105.6 (6)
C3–C2–C15	129.4 (7)	C11–C12–O2	103.7 (6)
C3–C2–O1	106.4 (6)	C13–C12–O2	106.8 (6)
C15–C2–O1	107.5 (6)	C12–C13–C14	119.4 (6)
C2–C3–C4	117.1 (7)	C12–C13–C17	101.8 (6)
C2–C3–C7	103.0 (6)	C14–C13–C17	101.6 (6)
C4–C3–C7	102.6 (6)	C13–C14–C15	104.9 (6)
C3–C4–C5	105.4 (7)	C2–C15–C14	120.4 (7)
C4–C5–C6	102.9 (6)	C2–C15–C16	103.3 (6)
C4–C5–C12	117.9 (6)	C14–C15–C16	101.6 (6)
C6–C5–C12	101.7 (6)	C15–C16–C17	104.9 (6)
C5–C6–C7	106.3 (6)	C15–C16–C20	106.6 (6)
C5–C6–C10	108.9 (6)	C17–C16–C20	102.8 (6)
C7–C6–C10	102.6 (6)	C13–C17–C16	106.4 (6)
C3–C7–C6	105.7 (6)	C13–C17–C18	107.3 (6)
C3–C7–C8	108.4 (6)	C16–C17–C18	102.5 (6)
C6–C7–C8	102.6 (6)	C11–C18–C17	96.7 (6)
C1–C8–C7	96.8 (6)	C11–C18–C19	107.6 (6)
C1–C8–C9	106.6 (6)	C17–C18–C19	103.3 (6)
C7–C8–C9	103.0 (6)	C18–C19–C20	93.3 (6)
C8–C9–C10	96.2 (6)	C1–C20–C16	98.7 (6)
C6–C10–C9	103.5 (6)	C1–C20–C19	106.2 (6)
C6–C10–C11	96.7 (6)	C16–C20–C19	104.7 (6)
C9–C10–C11	106.2 (6)	C2–O1–C21	116.1 (6)
C1–C11–C10	102.6 (6)	C12–O2–C22	117.4 (6)

slope of 1.155 indicates a slight, but steady, tendency toward too long bonds.

Crystallographic Section. Data were collected on a Syntex $P2_1$ automated diffractometer using Mo Kα graphite-monochromatized radiation. Three check reflections were monitored at 50-reflection intervals which for each compound exhibited no significant variation in intensity.

[1.1.1.1]Pagodane [Undecacyclo[9.9.0.0^{1,5}.0^{2,12}.0^{2,18}.0^{3,7}.0^{6,10}.0^{8,12}.0^{11,15}.0^{13,17}.0^{16,20}]eicosane (1)]. Single crystals were obtained by slow evaporation from dichloromethane. Crystal data and details are summarized in Table II. One hemisphere of reciprocal space ($h,\pm k,\pm l$) was sampled at room temperature. The compound crystallizes in the triclinic space group $P\bar{1}$, with an inversion point at the center of the molecule. Direct methods were employed to provide seven carbon positions, and difference Fourier synthesis was used to locate the other three carbon atoms. With calculated hydrogen positions, full-matrix least-squares refinement led to a final agreement factor of $R = 0.055$ for 1387 reflections with $I > 3\sigma(I)$. The bond distances and selected bond angles are compiled in Tables III and IV, respectively.

2,12-Dimethoxydecacyclo[9.9.0.0^{1,8}.0^{2,15}.0^{3,7}.0^{5,12}.0^{6,10}.0^{11,18}.0^{13,17}.0^{16,20}]eicosane (16). From slow evaporation from dichloromethane solution, a cubelike colorless crystal was isolated. Before the X-ray measurements, the crystal was coated with epoxy to prevent loss of cocrystallized solvent. The molecule crystallizes in the orthorhombic space group *Fdd*2; unit cell parameters and further details are given in Table II. Intensities of 2173 reflections were measured in one quadrant of reciprocal space ($h,k,\pm l$). Averaging of equivalent measurements resulted in a total of 913 unique reflections having intensities greater than $3\sigma(I)$. The coordinates of carbon and oxygen atoms of the compound were obtained by direct methods and those of the solvent atoms (C, Cl) from subsequent difference Fourier maps. In the least-squares refinement, all the non-hydrogen atoms were assigned anisotropic thermal parameters. After the calculated hydrogen positions were added, the final refinement resulted in the agreement factor $R = 0.066$ for 1220 reflections. Bond distances and selected bond angles of the molecule are listed in Tables V and VI.

[2.2.1.1]Pagodane [Undecacyclo[11.9.0.0^{1,6}.0^{2,14}.0^{2,20}.0^{3,8}.0^{7,12}.0^{9,14}.0^{13,17}.0^{15,19}.0^{18,22}]docosane (21)]. A cubelike colorless crystal was isolated from dichloromethane by slow evaporation of the solvent. Crystal parameters and other details are listed in Table II. Intensities of 1909 reflections were measured in one quadrant of reciprocal space ($h,k,\pm l$). The coordinates of all carbon atoms were obtained by direct methods. With calculated hydrogen positions, the final refinement resulted in an agreement factor of $R = 0.049$ for 1320 reflections with $I > 3\sigma(I)$.

Table VII. Experimental and Calculated Bond Distances (Å) for **21**

type	exptl	exptl (av)	MNDO	AM1	MINDO/3
C1–C2	1.562 (5)	1.560	1.600	1.591	1.639
C13–C14	1.557 (5)				
C1–C6	1.522 (5)	1.522	1.545	1.517	1.568
C2–C3	1.525 (5)				
C9–C14	1.519 (5)				
C12–C13	1.521 (5)				
C1–C13	1.551 (5)	1.549	1.584	1.579	1.615
C2–C14	1.546 (5)				
C1–C22	1.528 (5)	1.536	1.551	1.528	1.572
C2–C20	1.534 (5)				
C13–C17	1.536 (5)				
C14–C15	1.546 (5)				
C3–C4	1.528 (5)	1.528	1.542	1.512	1.535
C5–C6	1.520 (5)				
C9–C10	1.527 (5)				
C11–C12	1.537 (5)				
C3–C8	1.554 (5)	1.551	1.581	1.563	1.581
C6–C7	1.554 (5)				
C7–C12	1.551 (5)				
C8–C9	1.543 (5)				
C4–C5	1.546 (5)	1.543	1.541	1.518	1.525
C10–C11	1.539 (5)				
C7–C8	1.578 (5)	1.578	1.593	1.555	1.605
C15–C16	1.541 (5)	1.541	1.557	1.546	1.544
C16–C17	1.541 (5)				
C20–C21	1.536 (5)				
C21–C22	1.546 (5)				
C15–C19	1.550 (5)	1.549	1.576	1.560	1.576
C17–C18	1.543 (5)				
C18–C22	1.548 (5)				
C19–C20	1.555 (5)				
C18–C19	1.576 (5)	1.576	1.602	1.585	1.609

Table VIII. Selected Bond Angles (deg) for **21**

type	angle	type	angle
C1–C13–C12	106.6 (3)	C13–C17–C16	103.3 (3)
C1–C13–C14	90.0 (2)	C13–C17–C18	99.8 (3)
C1–C13–C17	104.8 (3)	C16–C17–C18	103.5 (3)
C12–C13–C14	109.8 (3)	C17–C18–C19	103.4 (3)
C12–C13–C17	130.4 (3)	C17–C18–C22	109.8 (3)
C14–C13–C17	104.1 (3)	C19–C18–C22	102.9 (3)
C2–C14–C9	106.5 (3)	C15–C19–C18	103.0 (3)
C2–C14–C13	90.2 (2)	C15–C19–C20	109.6 (3)
C2–C14–C15	108.4 (3)	C18–C19–C20	103.7 (3)
C9–C14–C13	111.2 (3)	C2–C20–C19	99.6 (3)
C9–C14–C15	130.2 (3)	C2–C20–C21	103.8 (3)
C13–C14–C15	103.1 (3)	C19–C20–C21	102.5 (3)
C14–C15–C16	103.5 (3)	C20–C21–C22	96.0 (3)
C14–C15–C19	99.7 (3)	C1–C22–C18	99.8 (3)
C16–C15–C19	103.6 (3)	C1–C22–C21	103.6 (3)
C17–C16–C15	95.5 (3)	C18–C22–C21	103.1 (3)

Tables VII and VIII contain the bond distances and selected bond angles.

Acknowledgment. Support of this work at USC by the National Institutes of Health and at Freiburg by the Deutsche Forschungsgemeinschaft, the Fonds der Chemischen Industrie, and the BASF AG is gratefully acknowledged.

Registry No. 1, 89683-62-5; **9**, 99828-64-5; **10**, 116725-79-2; **12**, 116725-80-5; **13**, 116725-81-6; **15**, 116725-82-7; **16**, 99808-96-5; **16** dihydroxy derivative, 108148-33-0; **18**, 107798-65-2; **19**, 107798-67-4; **21**, 107914-52-3; **24**, 111209-27-9; **29**, 116725-83-8; **30**, 116725-84-9; **31**, 704-02-9; **32**, 6707-86-4; **33**, 452-61-9; **34**, 277-10-1; **40**, 111160-98-6.

Supplementary Material Available: Tables of final atomic coordinates, anisotropic temperature factors, and calculated hydrogen positions for compounds **1**, **16**, and **21** (Tables A–J) (8 pages); observed and calculated structure factors for compounds **1**, **16**, and **21** (Tables K–M) (17 pages). Ordering information is given on any current masthead page. Z matrices and Cartesian coordinates of calculated geometries for molecules in Scheme I are available from us at UF.